Controlling chimera states in chaotic oscillator ensembles through linear augmentation

Anjuman Ara Khatun,[1] Haider Hasan Jafri,[1] and Nirmal Punetha[2,*]
[1]*Department of Physics, Aligarh Muslim University, Aligarh 202 002, India*
[2]*Department of Physics and Astrophysics, University of Delhi, Delhi 110007, India*

(Received 20 November 2019; accepted 7 March 2021; published 5 April 2021)

In this work, we show how "chimera states," namely, the dynamical situation when synchronized and desynchronized domains coexist in an oscillator ensemble, can be controlled through a linear augmentation (LA) technique. Specifically, in the networks of coupled chaotic oscillators, we obtain chimera states through induced multistability and demonstrate how LA can be used to control the size and spatial location of the incoherent and coherent populations in the ensemble. We examine basins of attraction of the system to analyze the effects of LA on its multistable behavior and thus on chimera states. Stability of the synchronized dynamics is analyzed through a master stability function. We find that these results are independent of a system's initial conditions and the strategy is applicable to the networks of globally, locally as well as nonlocally coupled oscillators. Our results suggest that LA control can be an effective method to control chimera states and to realize a desired collective dynamics in such ensembles.

DOI: 10.1103/PhysRevE.103.042202

I. INTRODUCTION

Chimera is an interesting collective state exhibited by oscillator ensembles where synchronized and desynchronized dynamics coexists in the system. In classical settings, chimera states emerge in the system as a result of nonlocal interactions when the ensemble of coupled identical phase oscillators spontaneously form two groups: one that exhibits synchronized motion while the other group remains desynchronized [1,2]. In general, however, these states can occur in a variety of oscillator ensembles with global and local coupling topologies as well [3–6]. Emergence of chimera states in various networks has been analyzed in order to understand, for example, unihemispheric and rapid eye movement sleep, ventricular fibrillation, coexistence of laminar and turbulent flows in fluids, robustness of synchronized power grids, and consensus formations in social networks [7]. Due to the widespread occurrence of this phenomenon, study of these interesting spatiotemporal patterns has found relevance in various disciplines, including neuroscience [8,9], biology [10,11], Josephson junction arrays [12], metronomes [13,14], and electrochemical systems [15,16].

In addition to the dynamical flows, chimera states have been known to exist in ensembles of time-discrete systems as well. Studies of several nonlocally coupled maps have analyzed the emergence of such hybrid states in discrete dynamical systems [17–21]. It has also been observed that ensembles of nonlocally coupled bistable systems, including maps and flows, with regular as well as chaotic dynamics have the ability to exhibit different types of chimera structures [18]. Recent studies have suggested that chimeric states can be created in a system of instantaneously coupled identical chaotic oscillators through induced multistability [22–24]. Here, the multistable behavior can be induced in the system via mutual coupling or driving, which causes the basins of the coexisting attractors to be completely intertwined [25], and leads to the emergence of stable chimera states for arbitrary initial conditions. The nature of the transitions leading to multistable behavior and corresponding basins of attraction have been analyzed previously to understand such chimeric behaviors [26,27].

An important aspect in the study of this curious spatiotemporal phenomenon, so-called chimera state, is related to its control. A number of studies have been dedicated to explore methods for controlling various features of chimera states; these include its stability, lifespan, basins of attraction, and the size and positions of coherent and incoherent domains [28–35]. Examples of such control strategies include remote pacemaker control [36], pinning [37], applying gradient dynamics in order to dynamically modulate the position of the coherent part of a chimera [38], influence of a block (or barrier) of excitable units [39], and a minimal coupling modification method [40]. In this work, we obtain chimera states in the network of coupled chaotic oscillators through induced multistability, and propose to implement a linear augmentation (LA) technique to control such chimeric states. Using this strategy, we show that the dynamics of a multistable ensemble and thus the chimera states can be controlled by coupling it to a linear system. It is known that LA is a powerful method for targeting fixed-point solutions [41], suppressing bistability [42], controlling the dynamics of drive-response systems [43], and regulating the dynamics of hidden attractors [44]. Additionally, this control scheme has the advantage that it allows one to achieve a desired response state in the ensemble without manipulating system parameters. Therefore it can be very useful to control chimera states emerging in the networks coupled with different topologies including global, nonlocal, and local coupling schemes.

*punethanirmal@gmail.com

 ©2021 American Physical Society

For our analysis, we consider a network of N mutually coupled identical chaotic oscillators. Dynamics of these oscillators is described by d state variables $\vec{\mathbf{X}} \in \mathbb{R}^d$, evolving according to the rule $\dot{\vec{\mathbf{X}}} = F(\vec{\mathbf{X}})$, and connected to other oscillators through one of these state variables. In such ensembles, chimera states can be created by inducing multistability in the system [23]. In the following, we discuss the emergence of chimera states in such ensembles, and demonstrate how these states can be efficiently managed using LA by simply connecting or augmenting oscillators of the networks to a linear system. This approach can be used to modify collective properties of the system, for example, to generate chimeras with coherent and incoherent domains of required size and spatial locations. One can also destroy chimeras and obtain a dynamical state where the oscillator population exhibits complete synchronization, cluster synchronization, or remains incoherent. We find, for appropriate choices of augmentation parameters, multistability can be suppressed in the system leading it to a desired collective state. The riddled basin of the unaugmented system also changes its properties as a result of linear augmentation. Further, one can verify the stability of such resulting states by examining the behavior of master stability function (MSF) [45–47].

The organization of the article is as follows. In the following Sec. II, we discuss the creation of chimera states through induced multistability in the globally coupled Lorenz oscillators and explain how LA can be used to control these states in Sec. III. Further, the effect of implementing LA control is analyzed by examining the change in basin of attractions and stability of the synchronized states through MSF in Sec. IV. We extend our study for both local and nonlocal coupling schemes in Sec. V and discuss how spatial location of synchronized and incoherent domains can be controlled in the chimeric population. This is followed by a summary and discussion in Sec. VI.

II. COLLECTIVE DYNAMICS OF THE NETWORK OF GLOBALLY COUPLED OSCILLATORS

In this section, we discuss how chimera states can be created in a network of coupled chaotic Lorenz systems through induced multistability. We consider an ensemble of N mutually coupled Lorenz oscillators described mathematically by the following equations:

$$\begin{aligned}
\dot{x}_i &= \rho(y_i - x_i),\\
\dot{y}_i &= \gamma x_i - y_i - x_i z_i,\\
\dot{z}_i &= x_i y_i - \beta z_i + \frac{\varepsilon_1}{(N-1)} \sum_i A_{ij}(z_j - z_i),
\end{aligned} \tag{1}$$

where the index $i = 1, 2, \ldots, N$. Oscillators are connected through z variables, and the connection topology is represented by the adjacency matrix $\boldsymbol{A}$. Its elements A_{ij} are either one or zero depending on whether or not the ith and jth oscillators are connected [48]. We consider the case of global coupling, for which $A_{ij} = 1$ for all $i \neq j$ and zero otherwise. Here, ε_1 represents the global coupling strength. Since the Lorenz system is invariant under the transformation $(-x_i, -y_i, z_i) \to (x_i, y_i, z_i)$, coupling through z_i variables preserves the symmetry of the system in the x_i, y_i planes [27]. The parameter values are taken as $\rho = 10$, $\gamma = 24.8$, and $\beta = 8/3$, such that the fixed points of the isolated oscillators $[\pm\sqrt{\beta(\gamma-1)}, \pm\sqrt{\beta(\gamma-1)}, \gamma - 1]$ [49,50] are unstable and the dynamics of each of the uncoupled systems is chaotic. For coupled oscillators, multiple attractors coexist in the system with dynamically different behaviors [23]. Figure 1 shows three different attractors C_-, C_+, and C_0 that are observed in the system, Eq. (1), for $N = 2$ oscillators at coupling strength $\varepsilon_1 = 0.08$. In this multistable region, the oscillators settle into one of these three attractors, which is determined by their initial conditions. It is observed that if oscillators in the ensemble settle into the attractors C_- and C_+, their dynamics is synchronized, while the dynamics of the oscillators settling on attractor C_0 is incoherent.

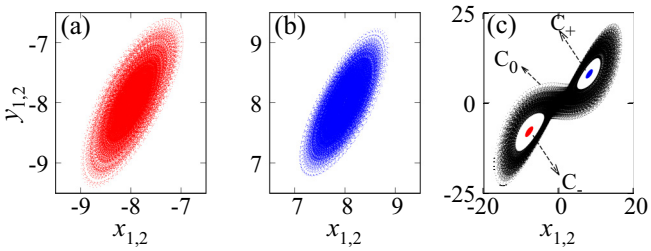

FIG. 1. In (a),(b),(c), we show multistable attractors C_-, C_+, C_0 observed in a system of coupled Lorenz oscillators at coupling strength $\varepsilon_1 = 0.08$.

Similar multistable attractors can be induced in the system of N globally coupled Lorenz oscillators [Eq. (1)] as well, and depending on their initial conditions, this gives rise to synchronized (dynamics in C_- and C_+) and desynchronized (dynamics in C_0) domains in the system. Therefore, the collective dynamics of Eq. (1) is a chimera as shown in Fig. 2 for $N = 100$ oscillators. Here, the chimera state consists of three

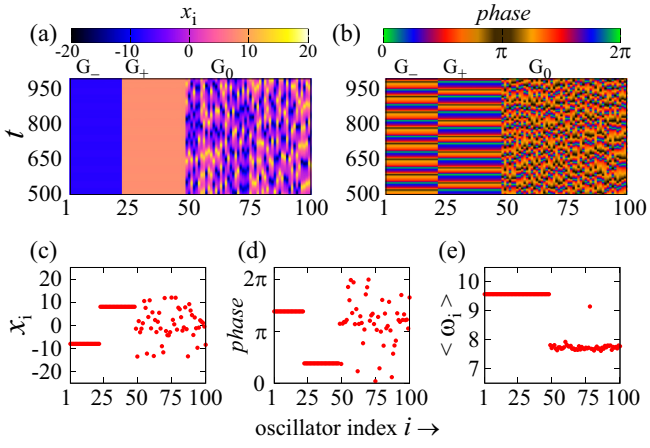

FIG. 2. Chimeric behavior in an ensemble of $N = 100$ coupled Lorenz oscillators at coupling strength $\varepsilon_1 = 0.08$. In the upper panel, the time evolutions of (a) x_i variables and (b) phases are shown. Oscillator groups asymptoting to the attractors $C_\mp$, C_0 are represented by $G_\mp$, G_0, respectively. Snapshots of the x variable and phases at time $t = 500$ are plotted in (c) and (d) while the time-averaged frequencies $\langle\omega_i\rangle$ of the oscillators are shown in (e).

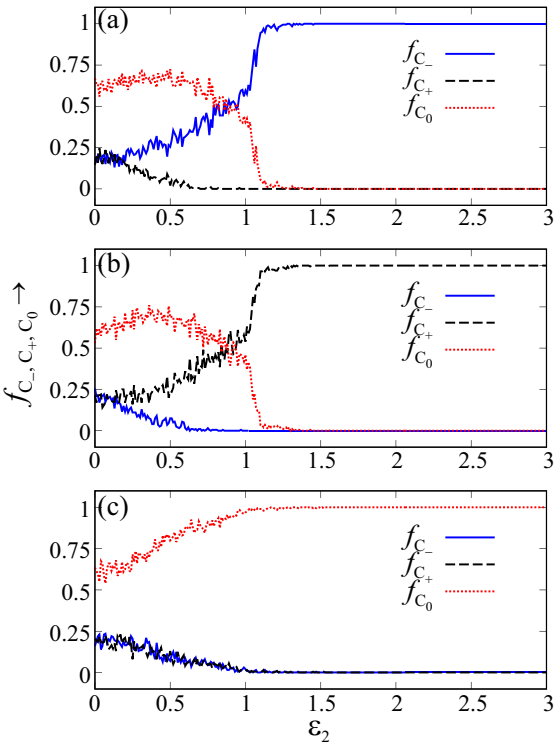

FIG. 3. Fraction of initial conditions going to attractors $C_{\mp,0}$ as a function of augmentation strength ε_2 are plotted with a solid blue line, a dashed black line, and a dotted red line, respectively. Control parameter is set to (a) $B \simeq B_-$, (b) $B \simeq B_+$, and (c) $B = B_0$. Results are obtained for a pair of coupled Lorenz systems with one augmented oscillator over 10^3 different initial conditions. Decay parameter $K = 3$ and coupling strength is fixed at $\varepsilon_1 = 0.08$.

distinct subpopulations ($G_{\mp,0}$) corresponding to oscillators settling into the three distinct attractors $C_{\mp,0}$ [23]. Figures 2(a) and 2(b) show the time evolution of the x_i variables and the phases, respectively [51], where one can observe the splitting of the entire population into three groups $G_\mp$ and G_0. While oscillators are synchronized in the first two groups $G_\mp$, the oscillators in the third group G_0 have incoherent dynamics. The snapshots of variables x_i at a fixed time is plotted in Fig. 2(c), confirming the synchronized and desynchronized behavior within the groups $G_\mp$ and G_0, respectively. Note that oscillators in the first two groups G_- and G_+ are in phase synchrony, as can be seen in the snapshots of the phases in Fig. 2(d). The synchronized dynamics of the groups $G_\mp$ can also be verified by average oscillator frequencies $\langle\omega_i\rangle$ as shown in Fig. 2(e). We calculate these average oscillator frequencies using $\langle\omega_i\rangle = \frac{2\pi Q_i}{\Delta T}$ [52]. Here Q_i is the number of maxima of the time series [53] of the ith oscillator within the time interval $\Delta T = 10^3$ units. Results are generated after removing initial transients for 10^6 iterations, i.e., 10^4 time units [54]. The frequencies shown here [Fig. 3(e)] are time-averaged values estimated from the number of maxima of the oscillator trajectories. Due to their averaged behavior, the frequencies of the incoherent oscillators, calculated on chaotic attractor C_0, have a range which is not so large; however, they are distinct enough to characterize incoherent population and differentiate it from the synchronized oscillators. Here, we see that rather than having a typical arc-shaped phase profile, which is observed in classical settings, the phases (and frequencies) of the oscillators in the coherent population are equal. This is similar to the behavior of the chimera populations originated from purely local or global coupling schemes, amplitude mediation, intensity induced or the ones observed in the multiplex or modular networks [3,22,55].

III. EFFECT OF LINEAR AUGMENTATION

Linear augmentation is a simple but powerful method to control the dynamics of a nonlinear dynamical system. By augmenting a linear system to a target, one can force the target system towards a given fixed point or destroy multistable attractors by merging of the unstable fixed points in the system [43]. In the following, we explain the LA method and discuss how it can be applied to our system of coupled chaotic oscillators in order to control its collective dynamics. A typical form for a linearly augmented system is given by

$$\begin{aligned}\dot{\vec{\mathbf{X}}} &= F(\vec{\mathbf{X}}) + \varepsilon\vec{\mathbf{W}},\\ \dot{\vec{\mathbf{W}}} &= -K\vec{\mathbf{W}} - \varepsilon(\vec{\mathbf{X}} - B).\end{aligned} \tag{2}$$

Here $\dot{\vec{\mathbf{X}}} = F(\vec{\mathbf{X}})$ represents the d-dimensional ($\vec{\mathbf{X}} \in \mathbb{R}^d$) nonlinear system which is to be augmented. $\dot{\vec{\mathbf{W}}} = -K\vec{\mathbf{W}}$ describes the dynamics of the d-dimensional linear system with $\vec{\mathbf{W}} = [w, 0, 0, 0 \ldots]^T$ and K is the decay parameter [56]. The term $\varepsilon(\vec{\mathbf{X}} - B)$ provides sustained oscillations to the linear system. $B = [b, 0, 0, 0 \ldots]^T$ is the control parameter of the augmented system. Its value is set close to the target fixed points of the system [41–43]. Here, superscript T indicates transpose of the matrix.

One can control the dynamics of a given set of oscillators by augmenting them to the corresponding linear systems. This augmentation results in a dynamical state with a desired property and does not affect the dynamics of the remaining oscillators present in the network. We couple x_i variables of a selected number of Lorenz oscillators, upon which we wish to implement control, to their corresponding linear systems as follows:

$$\begin{aligned}\dot{x}_i &= \rho(y_i - x_i) + \varepsilon_2 E_i w_i,\\ \dot{y}_i &= \gamma x_i - y_i - x_i z_i,\\ \dot{z}_i &= x_i y_i - \beta z_i + \frac{\varepsilon_1}{(N-1)}\sum_j A_{ij}(z_j - z_i),\\ \dot{w}_i &= -K w_i - \varepsilon_2 E_i(x_i - B).\end{aligned} \tag{3}$$

Here the parameters of Lorenz oscillators $\rho = 10$, $\gamma = 24.8$, $\beta = 8/3$ are the same as before. $i, j = 1, 2, 3, \ldots, N$. ε_2 is the feedback coupling strength or augmentation strength between the linear and the Lorenz system. The values E_i represent the connections between the oscillators in the ensemble and their corresponding linear systems: $E_i = 1$ if the ith oscillator is connected to the linear system and zero otherwise. For global coupling, the elements of the connectivity matrix are $A_{ij} = 1$ for $i \neq j$, $A_{ii} = 0$, as described earlier. We consider a

fixed value of decay parameter $K = 3$ for the linear systems throughout the article.

In Fig. 2, we see that the dynamics of the coupled oscillator ensemble is chimeric for the case without augmentation ($E_i = 0, \forall\, i$). To control this state, we apply LA to the system so that the behavior of the given set of oscillators (or the whole population) can be changed as desired. The final state of the augmented system depends upon the augmentation parameters, namely, decay parameter K, augmentation strength ε_2, and control parameter B. Morphologically, the attractors $C_{\mp}$ are formed due to chaotic modulation of the fixed points $\vec{\mathbf{X}}^*_{i_{\mp}}$ in the coupled systems [50]. Therefore, to achieve a preferential dynamics on one of these attractors, we set B to a value approximately equal to one of these fixed points. These fixed points can be evaluated by solving the equation of motion at the equilibrium, given by

$$\begin{aligned} \rho(y_i^* - x_i^*) &= 0, \\ \gamma x_i^* - y_i^* - x_i^* z_i^* &= 0, \\ x_i^* y_i^* - \beta z_i^* + \frac{\varepsilon_1}{(N-1)} \sum A_{ij}(z_j^* - z_i^*) &= 0. \end{aligned} \tag{4}$$

Solving these equations, we get three sets of equilibrium points as follows: the first one is the origin, i.e., $\vec{\mathbf{X}}^*_{i_0} \equiv (x^*_{i_0}, y^*_{i_0}, z^*_{i_0}) \equiv (0, 0, 0)$, and another two sets are given by $\vec{\mathbf{X}}^*_{i_{\mp}} \equiv (x^*_{i_{\mp}}, y^*_{i_{\mp}}, z^*_{i_{\mp}}) \equiv [\mp\sqrt{\beta(\gamma-1)}, \mp\sqrt{\beta(\gamma-1)}, \gamma - 1]$.

We fix the decay parameter value K and connect a selected number of oscillators to the corresponding linear systems with augmentation strength ε_2. Further, the following choices can be made for B: $B \simeq B_{\mp} = x^*_{i_{\mp}} = \mp\sqrt{\beta(\gamma-1)}$ and $B = B_0$, $x^*_{i_+} \ll B_0 \ll x^*_{i_-}$. For the choice $B \simeq B_{\mp}$, the system dynamics moves to the attractor $C_{\mp}$ and for $B = B_0$, the system dynamics evolves towards the attractor C_0. Note that control parameter B is approximately equal to $B_{\mp}$, since for $B = B_{\mp}$, the system shows a fixed point $x^*_{i_{\mp}}$ dynamics.

In the following, we first demonstrate the effects of LA in a simplest system of two coupled oscillators by connecting one of them to a corresponding linear system ($E_1 = 1$, $E_2 = 0$). Then we apply an augmentation method for controlling the dynamics of large ensembles ($N = 100$) as well. To see how LA modifies the resulting dynamics of the system, we trace the fraction of initial conditions settling into different attractors f_{C_-}, f_{C_+}, and f_{C_0} as a function of augmentation strength ε_2. These fractions are calculated by evolving the system of $N = 2$ oscillators for large initial conditions for all three choices of control parameter $B \simeq B_{\mp}$ and $B = B_0$, and the results are plotted in Fig. 3. As discussed for the case without LA ($\varepsilon_2 = 0$), coupled oscillator systems have three coexisting attractors $C_{\mp}, C_0$ at coupling strength $\varepsilon_1 = 0.08$. Since LA does not change the intrinsic system characteristics, these attractors persist for the augmented system ($\varepsilon_2 > 0$) as well. However, the fraction of initial conditions settling into these attractors can be controlled as a function of augmented strength ε_2, which is shown in Fig. 3 by solid blue, dashed black, and dotted red curves, respectively. Choosing a control parameter as required, i.e., by setting $B \simeq B_{\mp}$ and $B = B_0$, asymptotic dynamics of the oscillators can be modified and one can control the fraction of initial condition settling into a specific attractor. In Fig. 3, the fractions $f_{C_{\mp,0}}$ for the case

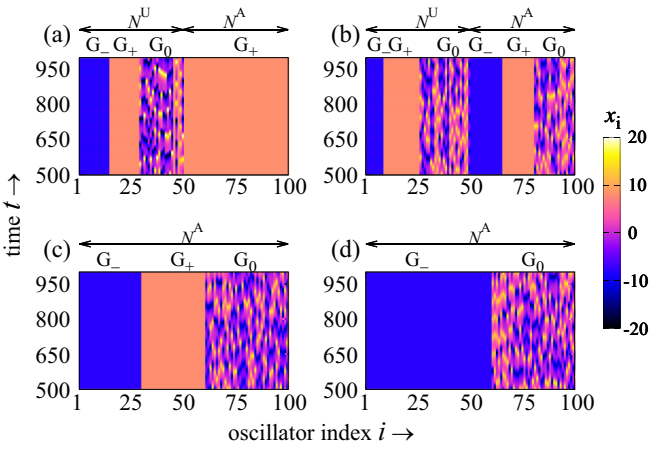

FIG. 4. Time evolution of the x variables for the ensemble of $N = 100$ oscillators. These space-time plots show the examples of control through linear augmentation for the cases when half (upper panel) and all (lower panel) oscillators are augmented. For $N^A = 50$, the first 50 unaugmented oscillators exhibit chimeric behavior with three coexisting $G_{\mp,0}$ groups. By appropriately choosing a control parameter, the rest of the oscillators are entrained towards a single group, G_+ in (a), or multiple (all three) groups $G_{\mp,0}$ in (b). When $N^A = 100$, the whole population can be entrained towards (c) three groups $G_{\mp,0}$ of the desired sizes, or (d) one synchronized G_- and one desynchronized group G_0 of the desired sizes. The parameters $\varepsilon_1 = 0.08$, $K = 3$, and $\varepsilon_2 = 2.5$.

without LA can be seen at $\varepsilon_2 = 0$. We can see the changes in these fractions as a result of LA when control parameter is taken as $B \simeq B_{\mp}$, $B = B_0$ in Figs. 3(a)–3(c), respectively.

One can use this strategy to obtain a desired collective state in an ensemble of oscillators as well. To illustrate the results of such control in a system of $N = 100$ oscillators [Eq. (3)], we fix the augmentation strength at $\varepsilon_2 = 2.5$ and explore its collective dynamics when ((i)) only a fraction of the population is augmented and (ii) when we apply the LA method to the whole population.

Case (i). In this case, linear augmentation is applied to a part of the oscillator population. Only half of the Lorenz oscillators are considered for augmentation and connected to the corresponding linear systems, i.e., $N^A = 50$. The remaining half $N^U = N - N^A = 50$ are kept unaugmented. This strategy, where only a selected fraction of oscillators are augmented, can be useful for controlling the size of different groups in the chimeric population. For example, in Figs. 4(a) and 4(b), the unaugmented set $N^U = 50$ exhibits the chimera state as before, where the population splits into three groups $G_{\mp,0}$, with two synchronized clusters and one desynchronized cluster. However, by choosing control parameter $B \simeq B_+$, the asymptotic dynamics of the remaining augmented oscillators can be made to settle on the attractor C_+, resulting in the formation of the group represented by G_+ and thus increasing the size of this population [see Fig. 4(a)]. Similarly, when we consider $B \simeq B_-$ or $B = B_0$, the augmented population follows the dynamics of the groups G_- (synchronized) or G_0 (desynchronized), respectively, corresponding to the attractors C_- or C_0. Thus, by appropriately choosing the control parameter B value, one can entrain a selected number of augmented

TABLE I. Possible choices of control parameter B.

Control parameter B	Dynamical states
$B \simeq B_-$	Coherent cluster G_-
$B \simeq B_+$	Coherent cluster G_+
$B = B_0$	Incoherent cluster G_0
$B \simeq B_-, B \simeq B_+$	Coherent clusters G_- and G_+
$B \simeq B_-, B = B_0$	Chimera with G_- and G_0
$B \simeq B_+, B = B_0$	Chimera with G_+ and G_0
$B \simeq B_-, B \simeq B_+, B = B_0$	Chimera with three clusters $G_{\mp,0}$

oscillators towards one of the groups to increase its size. When a single control parameter is selected for the entire augmented population, one can increase the size of only one of the clusters. However, the size of all the groups $G_{\mp,0}$ can be controlled at once by considering multiple B values simultaneously. This is shown in Fig. 4(b), where we consider $B \simeq B_\mp$ and $B = B_0$ simultaneously for augmented oscillators. As a result, the augmented oscillators split into three groups represented by $G_{\mp,0}$, containing, respectively, 15, 15, and 20 oscillators in each set.

Case (ii). This strategy, where we augment all the oscillators in the ensemble to corresponding linear systems, provides the maximum control over the collective dynamics. Considering single or multiple value(s) of the control parameter B for the entire population, one can either entrain all oscillators towards a single group destroying the chimera state, or obtain chimeras as a resulting dynamics with desired cluster sizes. An example is shown in Fig. 4(c) where different B values (B_-, B_+, and B_0) are considered simultaneously to individually control synchronized (both G_- and G_-) and desynchronized (G_0) populations of the chimera state. Similarly, in Fig. 4(d), we take $B \simeq B_-$ and $B \simeq B_0$ simultaneously to force the oscillator dynamics towards the attractors C_- and C_0, thus forming the two groups G_- and G_0. Consequently, the resulting dynamics is a chimera state as desired with two clusters (G_- and G_0), containing 60 and 40 oscillators in each group.

One can use these strategies to obtain a desired collective state in the system. For example, in Table I, we show different possibilities for the choices of control parameter B, and the dynamical states resulting from these choices. Note that here we mainly use ε_2 and B to achieve a desired dynamics. The decay parameter K does not directly affect the selection of the resulting attractor. The linear system has intrinsically decaying dynamics (decay rate K), which combined with the feedback signal from the augmented oscillators leads to oscillatory behavior. It is observed that for higher values of decay parameter K, the system typically goes to attractors $C_\mp$ with smaller amplitudes, and it tends to stay on bigger attractor C_0 when the decay rate is relatively small. The final state depends on the selection of the target attractor determined by B, and how much strength we use for augmentation, which is tuned by ε_2. We find that these are more efficient parameters for controlling chimera states. However, K should be selected in such a way that it allows optimum control through these augmentation parameters.

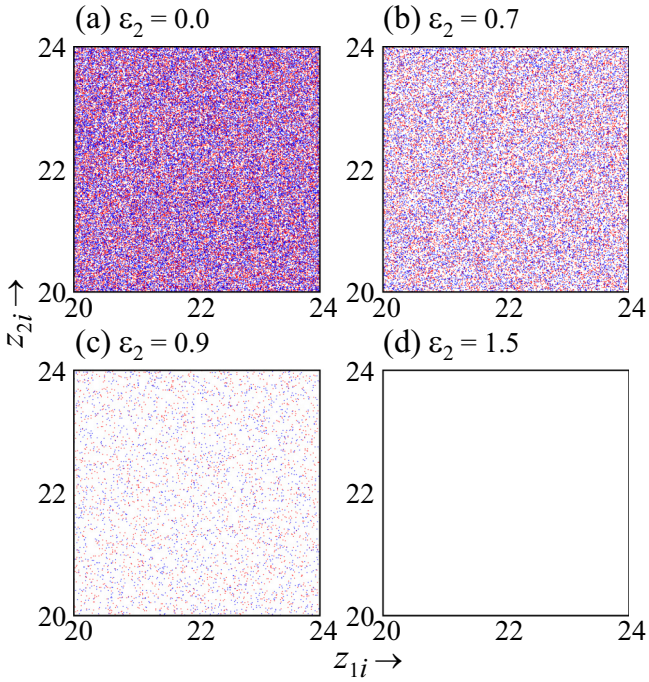

FIG. 5. Basin of attraction of the system of two coupled Lorenz oscillators at different augmentation strengths ε_2. Basins are calculated for initial conditions in z variables, i.e., z_{1i}, z_{2i} space in the interval [20, 24]. Initial values of x, y, and w variables are fixed, i.e., $x_{1i} = x_{2i} = 1$, $y_{1i} = y_{2i} = 1$, and $w_{1i} = w_{2i} = 1$. The initial conditions evolving towards attractors $C_\mp$ and C_0 are represented by red (light gray), blue (dark gray), and blank regions, respectively. Parameters $\varepsilon_1 = 0.08$, $B = B_0$, $K = 3$ are fixed.

IV. ROBUSTNESS OF DIFFERENT STATES BEFORE AND AFTER LINEAR AUGMENTATION

We consider an ensemble of coupled chaotic oscillators where the chimera state appears as a result of multistability. It is observed that the attractors $C_\mp$ and C_0 coexist in the system and within these attractors, the dynamics is quite different: the oscillators from the ensemble settling into attractors $C_\mp$ show synchronized behavior while the oscillators asymptoting to C_0 remain incoherent. The basin of attraction of these multistable attractors is intermingled and shows riddling [26,27]. Due to such complex basin structure, any two oscillators starting with even nearby initial conditions also have nonzero probability of settling into different attractors. As a result, for randomly chosen initial conditions, the oscillator ensemble organizes itself into three distinct subpopulations (two synchronized clusters and one desynchronized cluster $G_{\mp,0}$) leading to the chimeric dynamics. In Figs. 5(a)–5(d), we plot the basin of attraction at different augmentation strengths in order to illustrate the change in its properties due to the LA. The basin for the unaugmented system ($\varepsilon_2 = 0$) is riddled and completely interwoven in a complex manner as seen in Fig. 5(a). For this case, it is expected that two randomly selected nearby initial conditions may asymptote to different dynamical behaviors (synchronized and desynchronized) suggesting the emergence of chimera states for random [27,57] or quasirandom [58] initial conditions. However, for the augmented system, the

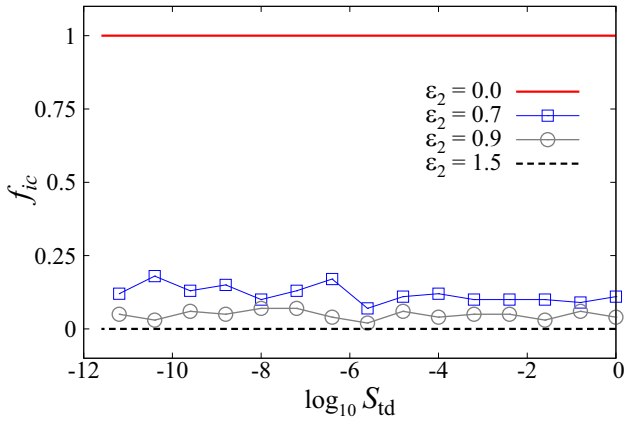

FIG. 6. Variation in the fraction of initial-condition pairs going to different attractors f_{ic} as a function of transversal distance $S_{\rm td} = |z_1 - z_2|$ at different augmentation strengths ε_2. For each transverse distance value $S_{\rm td}$, corresponding fraction $f_{\rm ic}$ is calculated from 10^3 different initial-condition pairs. Parameters and initial conditions are the same as in Fig. 5.

riddled nature of the basin gradually disappears with increasing augmentation strength ε_2 [Figs. 5(b) and 5(c)], and for its large values, only the basin of the desired attractor (selected through the control parameter B) remains in the domain [see Fig. 5(d)].

In Fig. 6, we examine the fraction of nearby initial-condition pairs $f_{\rm ic}$ settling on different attractors as a function of transversal distance $S_{td} = |z_1 - z_2|$ from the synchronization manifold [26,27]. Taking control parameter $B = B_0$, we calculate the fraction $f_{\rm ic}$ for different augmentation strengths ε_2 in order to observe the effect of LA on the basin properties. In the absence of LA ($\varepsilon_2 = 0.0$), the probability that nearby initial-condition pairs lead to distinct attractors is extremely high ($f_{\rm ic} \simeq 1$). However, as one increases augmentation strength ε_2, $f_{\rm ic}$ decreases indicating that a lesser number of nearby initial-condition pairs go to different attractors. For large ε_2 values, depending on the choice of control parameter (here, $B = B_0$), all initial conditions lead to a single attractor (here, C_0), and therefore the fraction $f_{\rm ic} = 0$ as can be seen in Fig. 6.

Next, we perform a MSF analysis for our system, which is a powerful technique to determine the stability of the synchronized dynamics in a network [45,46]. To examine the robustness of the synchronized states in our augmented system, we evaluate MSF for the ensemble of N coupled oscillators. We obtain the block-diagonal variational equation in which each block has the same form, and calculate the largest Lyapunov exponent of this variational equation. One can write a network of N coupled oscillators as

$$\frac{d\vec{\mathbf{X}}_i}{dt} = \mathbf{F}(\vec{\mathbf{X}}_i) - \varepsilon \sum_{j=1}^{N} G_{ij}\mathbf{H}(\vec{\mathbf{X}}_j), \tag{5}$$

where ε is a global coupling parameter, $\mathbf{H}(\vec{\mathbf{X}})$ is a coupling function, and $\mathbf{G}$ represents a coupling matrix determined by the connection topology. $\mathbf{G}$ has a zero or a constant row-sum to ensure the existence of a synchronization manifold. The variational equations

$$\frac{d\delta\vec{\mathbf{X}}_i}{dt} = \mathbf{DF}(\mathbf{s}) \cdot \delta\vec{\mathbf{X}}_i - \varepsilon \sum_{j=1}^{N} G_{ij}\mathbf{DH}(\mathbf{s}) \cdot \delta\vec{\mathbf{X}}_j \tag{6}$$

govern the time evolution of the set of infinitesimal perturbation vectors about the synchronous solution $\mathbf{s}$. The generic form of all decoupled blocks is then given by

$$\frac{d\delta\mathbf{y}}{dt} = [\mathbf{DF}(\mathbf{s}) - \kappa\mathbf{DH}(\mathbf{s})] \cdot \delta\mathbf{y}, \tag{7}$$

where κ is a normalized coupling parameter. The largest Lyapunov exponent for this equation $\lambda_M(\kappa)$ gives the MSF which describes the linear stability of the synchronized dynamics as a function of coupling parameter κ. Its positive, negative, and zero values correspond to the unstable, stable, and marginally stable synchronized states, respectively.

The oscillator ensemble considered here shows multistable behavior with coexisting attractors $C_{\mp,0}$. To examine the stability of the synchronized state with such multistability, it is necessary to calculate the MSF corresponding to the motions on each coexisting attractor [47]. Therefore, we calculate λ_M as a function of coupling strength ε_1 for all three attractors present in the unaugmented system, and the results are shown in Fig. 7(a). We observe, for smaller values of ε_1, the MSF is always positive for all three attractors $C_{\mp,0}$ shown by red squares, green circles, and blue triangles, respectively. This indicates that the motion on all attractors $C_{\mp,0}$ is desynchronized at these parameter values. As ε_1 is increased, the MSF for different attractors can take negative and positive values indicating both stable and unstable nature of the synchronized dynamics [e.g., see Fig. 7(a) when $\varepsilon_1 > 0.05$]. In this region, depending upon the attractor on which the motion takes place, both synchronized and incoherent motions are possible.

Similar to Fig. 7(a), the results for the augmented system are shown in Figs. 7(b)–7(d), where we plot the variation of MSF, λ_M, with augmentation strength ε_2 for three different choices of control parameter $B = B_{\mp,0}$, with $K = 3$ and $\varepsilon_1 = 0.08$. Here, the dynamics depends on the control parameter B of the linear system and becomes completely independent of the initial conditions with strong augmentation strength (see Fig. 5). However, for small ε_2 values (e.g., $\varepsilon_2 \lesssim 1.25$), all three attractors exist where both positive and negative values of λ_M can be observed. For this case, the augmentation strength is not strong enough to steer the system dynamics towards the desired attractor(s) and the control is not very efficient. As one increases ε_2, either a negative or a positive value of λ_M is observed depending upon the choice of control parameter: when $B \simeq B_{\mp}$, MSF becomes negative indicating the stabilization of synchronized dynamics on attractors $C_{\mp}$, and the choice $B = B_0$ leads to a desynchronized dynamics on attractor C_0 and positive λ_M values. These results suggest that using LA one can stabilize attractors $C_{\mp}$ with synchronized dynamics, or can destroy these attractors leading the system towards C_0 with incoherent behavior.

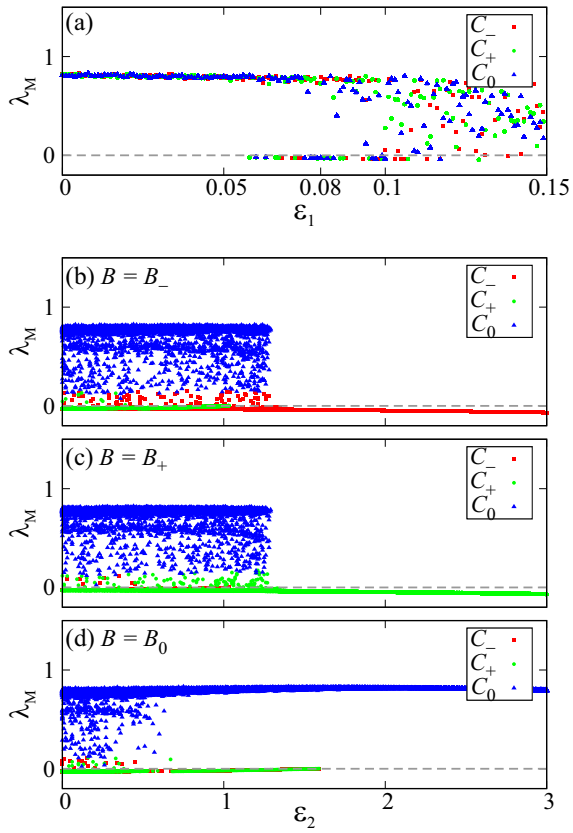

FIG. 7. For an ensemble of coupled Lorenz oscillators, the variation of MSF, λ_M, for the unaugmented system as a function of coupling strength ε_1 is plotted in (a). Here, red squares, green circles, and blue triangles represent λ_M values corresponding to the attractors $C_{\mp,0}$, respectively. (b)–(d) are the results for augmented system, where λ_M is plotted as a function of augmentation strength ε_2 for different choices of control parameter $B \simeq B_-$ (b), $\simeq B_+$ (c), and $= B_0$ (d). Parameters $K = 3$ and $\varepsilon_1 = 0.08$. Results are obtained for 100 different initial conditions.

V. LINEAR AUGMENTATION IN LOCALLY AND NONLOCALLY COUPLED FLOWS

In this section, we expand our analysis for locally and nonlocally coupled Lorenz systems and apply LA to control the collective behavior of such populations. The equation of motion for coupled identical Lorenz oscillators for such cases is written as

$$\begin{aligned}\dot{x}_i &= \rho(y_i - x_i),\\ \dot{y}_i &= \gamma x_i - y_i - x_i z_i,\\ \dot{z}_i &= x_i y_i - \beta z_i + \frac{\varepsilon_1}{2p}\sum_{j=(i-p)}^{(i+p)} A_{ij}(z_j - z_i),\end{aligned} \tag{8}$$

with index $i = 1, 2, 3, \ldots, N$, N being the number of oscillators. Here, each oscillator in the ensemble is coupled symmetrically with $2p$ nearest neighbors (p to its left, and p to its right) with coupling strength ε_1. Bearing to the network, one can define a parameter $r = p/N$ as the coupling radius [2]. For example, when $p = 1$, oscillators are coupled to its nearest neighbors only, referring to the locally coupled scenario with coupling radius $r = 1/N$. For the case of global coupling, all the oscillators are connected to each other; then $p = (N - 1)/2$ or $\approx N/2$ depending on whether N is odd or even, and the corresponding coupling radius $r = (N - 1)/2N \approx 0.5$. A value of r between these limits represent the case of nonlocal coupling [59,60]. In our case of $N = 100$ oscillators, $p = 1$ (i.e., $r = 0.01$) represents the local (nearest-neighbor) coupling, while $p = 35$ (i.e., $r = 0.35$) represents that each oscillator is connected to 70 (35 in each direction) oscillators, which implies a nonlocal coupling scheme. Here, we discuss controlling chimera states both for locally ($r = 0.01$) and nonlocally ($r = 0.35$) coupled flows. In order to identify different dynamical states present in the network, we make use of a qualitative measure called "strength of incoherence" (SI), which is based on the standard deviation of the nearby variables as described in the literature [61]. For this calculation, the state variables given in Eq. (8) are transformed as $\mathbf{u}_i = \mathbf{x}_{i+1} - \mathbf{x}_i$, where $\mathbf{x}_i = [x_{1,i}, x_{2,i}, \ldots, x_{d,i}]^T \in \mathbb{R}^d$. The local standard deviation of the transformed state is then given by

$$\sigma_l(m) = \left\langle \sqrt{\frac{1}{n}\sum_{j=n(m-1)+1}^{mn} [u_{l,j} - \langle u_l\rangle]^2} \right\rangle_t, \tag{9}$$

where the total number of oscillators is divided into M bins with $n = N/M$ equal length, $m = 1, 2, \ldots, M$ and $l = 1, 2, \ldots, d$. The quantity $\langle \cdots \rangle_t$ denotes average over time. This gives the measure SI defined as

$$\mathrm{SI} = 1 - \frac{1}{M}\sum_{m=1}^{M} \Theta[\delta - \sigma_l(m)], \tag{10}$$

where Θ is a heavyside step function and δ is a small predefined threshold. SI takes the values SI = 1, SI = 0, and $0 <$ SI < 1 for incoherent, coherent, and chimera or multichimera states, respectively.

In Fig. 8, we show the behavior of SI as a function of coupling ε_1 and depict the observation of chimeric behavior in *unaugmented* locally and nonlocally coupled oscillator ensembles. We consider a system of $N = 100$ oscillators with coupling radius $r = 0.01$ and 0.35 for local and nonlocal couplings, respectively [60]. For both types of coupling schemes, we find that chimera states can be observed in the system when the coupling strength is approximately $\varepsilon_1 > 0.05$. This is indicated by the measure SI being $0 <$ SI < 1 for this parameter range, and verified in Figs. 8(a) and 8(d) where corresponding space-time plots are shown (using x_i variables) at $\varepsilon_1 = 0.08$.

In order to control the resulting dynamics of these ensembles, a desired number of oscillators from the ensemble are augmented to the corresponding linear systems. This augmented system is given by

$$\begin{aligned}\dot{x}_i &= \rho(y_i - x_i) + \varepsilon_2 E_i w_i,\\ \dot{y}_i &= \gamma x_i - y_i - x_i z_i,\\ \dot{z}_i &= x_i y_i - \beta z_i + \frac{\varepsilon_1}{2p}\sum_{j=(i-p)}^{(i+p)} A_{ij}(z_j - z_i),\\ \dot{w}_i &= -K w_i - \varepsilon_2 E_i (x_i - B).\end{aligned} \tag{11}$$

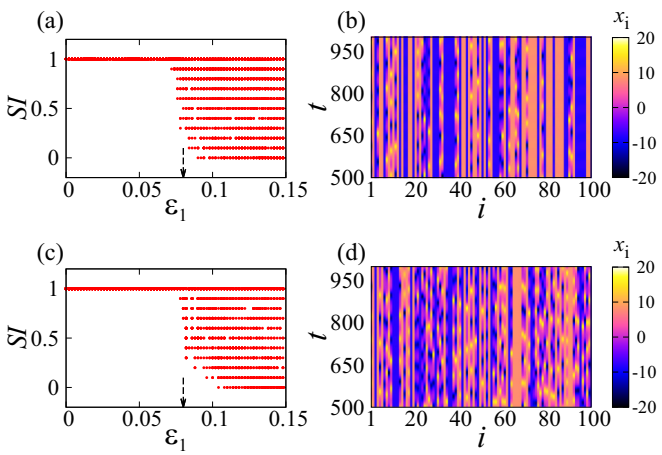

FIG. 8. Chimeric dynamics in locally (upper panel) and nonlocally (lower panel) coupled oscillator ensembles without LA. In the left panel, the strength of incoherence SI is plotted as a function of coupling strength ε_1 for (a) local and (c) nonlocal coupling schemes. Corresponding space-time plots are shown in the right panel for (b) locally and (d) nonlocally coupled systems at fixed coupling $\varepsilon_1 = 0.08$ (indicated by dashed arrows in the left panel). Calculation of SI is done by evolving the system for 100 different initial conditions at each ε_1 value.

Now, for the locally coupled oscillator system, we consider $p = 1$, i.e., $r = 0.01$, and show how the collective dynamics of such ensembles can be controlled using the LA technique. These results are illustrated in Fig. 9 where we present examples of controlling chimera states using (i) a fraction of the population and (ii) the entire population for augmentation.

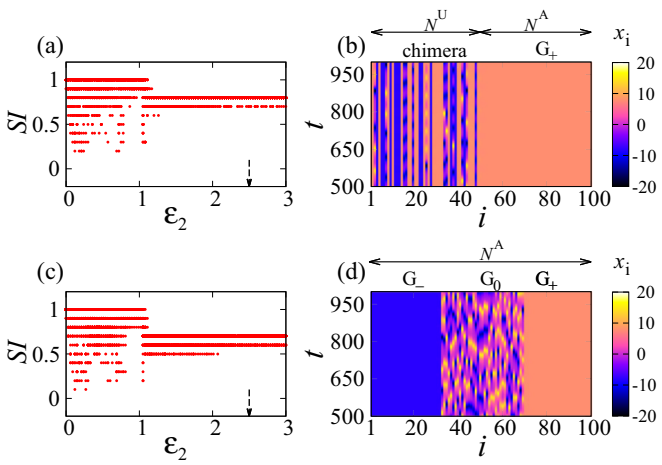

FIG. 9. Controlling chimera states through LA in locally coupled oscillators ($r = 0.01$). The strength of incoherence SI as a function of augmentation strength ε_2, and space-time plots are shown in the left and right panels, respectively. Depending on the number of augmented oscillators, two cases are shown: (i) $N^A = 50$ [in upper panels (a) and (b)], and (ii) $N^A = 100$ [in lower panels (c) and (d)]. Space-time plots are shown for a fixed augmentation strength $\varepsilon_2 = 2.5$, indicated by dashed arrows in the left panel. Calculation of SI is done by evolving the system for 100 different initial conditions at each ε_2 value.

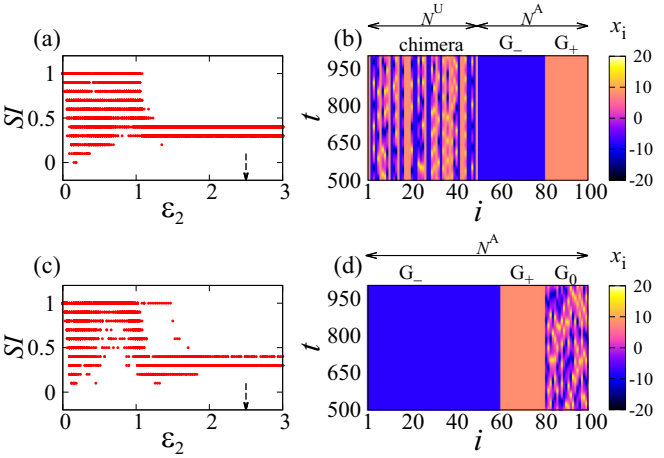

FIG. 10. Controlling chimera states through LA in nonlocally coupled oscillators ($r = 0.35$). The strength of incoherence SI as a function of augmentation strength ε_2, and space-time plots are shown in the left and right panels, respectively. The two cases shown are (i) $N^A = 50$, in (a) and (b); and (ii) $N^A = 100$, in (c) and (d). Space-time plots are shown for a fixed augmentation strength $\varepsilon_2 = 2.5$, indicated by dashed arrows in the left panel. Calculation of SI is done by evolving the system for 100 different initial conditions at each ε_2 value.

For both of these cases, the values of SI were calculated as a function of augmentation strength ε_2, and the results are shown in Figs. 9(a) and 9(c) for an ensemble of 100 locally coupled oscillators at parameters $\varepsilon_1 = 0.08$ and $K = 3$. We see in Fig. 9(b) that by appropriately choosing the control parameter B, one can force the dynamics of locally coupled oscillators towards a desired group; G_+ in this example. Further, by considering multiple B values simultaneously, one can control the size and location of the synchronized and desynchronized clusters, as depicted in Fig. 9(d) where the chimera state with clusters of sizes 30 : 40 : 30 is generated.

A similar control strategy can be applied for nonlocally coupled oscillator ensembles as well. The results for this case are shown in Fig. 10 for the system of $N = 100$ oscillators with nonlocal coupling $p = 35$ (i.e., $r = 0.35$) at $\varepsilon_1 = 0.08$, $K = 3$. When the population is partially augmented ($N^A = 50$), we use control parameter $B \simeq B_-$ for a group of 30 oscillators and $B \simeq B_+$ for the remaining 20. Such LA control leads to the entrainment of these populations towards the dynamics of G_- and G_+, respectively, as can be seen in Fig. 10(b). For the case when $N^A = 100$ [Fig. 10(d)], control parameters $B \approx B_-$, $B \approx B_+$, and $B = B_0$ are simultaneously used for augmenting, say, 60, 20, and 20 oscillators in order to obtain clusters G_-, G_+, and G_0 of sizes 60, 20, and 20, respectively. The spatial locations of these groups can be controlled by appropriately choosing control parameter B and the position of the oscillators that are to be augmented. These results show that with LA, one can easily control the size and spatial location of the chimera states and force the desired number of oscillators to follow a particular dynamics in a system of globally, locally, as well as nonlocally coupled oscillator ensembles.

VI. CONCLUSION

In this work, we examine the emergence of dynamical chimeras in coupled chaotic flows, and show how these states can be controlled through linear augmentation. By selectively switching on the couplings between the coupled flows and the corresponding linear systems, one can effectively control the resulting collective dynamics. Since the control in this case takes place at the level of every oscillator unit, it is possible to control individual oscillator dynamics and hence control the spatial locations in the chimera states. Our results suggest that by choosing appropriate values of augmentation parameters B, K, and ε_2, it is possible to shift the selected number of oscillators from one state to another desired state. With LA, one can force a selected oscillator population to settle into a single or multiple attractor(s), which can result in the appearance of both synchronized or desynchronized clusters in the ensemble. Further, we show that these observations are valid for all types of coupling mechanisms including global, local, and nonlocal interactions where chimera states are created through induced multistability. In unaugmented oscillators, we observe that the basin of attraction of coexisting attractors is of riddled nature. However, when oscillators are connected to the linear systems, i.e., with LA, riddling is reduced and chimeric behavior of the population can be regulated. The riddling disappears when multistablity is destroyed using LA control to achieve a target dynamics. For very large augmentation strengths, the basin of one of the attractors is found to be dominated, thus destroying the chimeric nature of the system. The behavior of the master stability function confirms the stabilization of synchronized state in the ensemble. MSF can have both positive (unstable synchrony) and negative (stable synchrony) values corresponding to different attractors present in the system with different synchronization properties.

LA is used to control multistable dynamics of the systems by targeting its fixed points and forcing the dynamics towards a particular attractor. Thus, only one of the attractors remains in the augmented system, destroying its multistable nature. This transition has earlier been described by the "boundary crisis" [42]. In our system, we target specific attractor(s) to control the chimera population. Our results suggest that the fraction of oscillators $f_{C_{\mp,0}}$, going towards the targeted attractor, as a function of augmentation strength gradually increases to one (see Fig. 3). This maximum value indicates that all initial conditions in the basin asymptote to a selected attractor. One can expect similar basin behavior for other systems where LA results in the disappearance of multistable behavior and leads to a single attractor dynamics.

Our results suggest that LA is helpful for controlling the size of the subpopulation and spatial locations of the synchronized and desynchronized clusters in the chimera states. The results presented here are quite general in the sense that they can be applied to the ensemble of oscillators where chimera states can be induced through multistability; examples include the ensembles of Rössler and Chua oscillators. Apart from globally coupled oscillators, we show that the LA technique can be applied to control the collective dynamics of the ensemble of locally and nonlocally coupled systems as well. With this technique, we can control the system dynamics through external parameters (parameters of the linear system), which are easily accessible. The simple technique using a linear system, in general, can be helpful in engineering collective dynamics of coupled networks where internal parameters are not accessible. There are instances, namely, in power grid [62,63] and neuronal systems [11,64,65] where it is difficult to access internal parameters of the system. In such cases, one may implement a simple linear augmentation technique to ensure an effective control over the collective dynamics of the system.

In general, chimera states are known to appear in oscillator ensembles when some degree of nonuniformity (in the coupling, topology, or parameters) is introduced in the system [7]; for example, with nonlocal (or variable) coupling, nonzero phase-lag parameter, modular networks, or due to the presence of time delay in the system. In this case, however, chimera states are obtained without such "heterogeneities": we induce multistability, and the synchronization properties of these multiple attractors are used to obtain chimera states in the chaotic oscillator ensembles. Thus the mechanism of emergence of chimera in this case is different from the classical scenarios where it is observed with nonlocal coupling. The strategies to control chimera states for these cases, therefore, are also different. Here we show linear augmentation, which is a powerful technique to control multistable dynamics, is quite effective in achieving desired state(s) in our system. Note that the effectiveness of LA is sensitive to the augmentation parameters, the class of oscillatory systems, the stationary solutions to be stabilized, as well as the way the systems are augmented [66]. Here, however, we find this control strategy is quite robust and the chimera population thus obtained is stable in the presence of perturbations and noise [67].

ACKNOWLEDGMENTS

A.A.K. and H.H.J. acknowledges University Grants Commission (UGC), India for the financial support. We also thank Ram Ramaswamy for useful discussions.

[1] Y. Kuramoto and D. Battogtokh, Nonlinear Phenom. Complex Syst. **5**, 380 (2002).
[2] D. M. Abrams and S. H. Strogatz, Phys. Rev. Lett. **93**, 174102 (2004).
[3] G. C. Sethia and A. Sen, Phys. Rev. Lett. **112**, 144101 (2014).
[4] G. C. Sethia, A. Sen, and F. M. Atay, Phys. Rev. Lett. **100**, 144102 (2008).
[5] O. E. Omel'chenko, Y. L. Maistrenko, and P. A. Tass, Phys. Rev. Lett. **100**, 044105 (2008).
[6] A. Yeldesbay, A. Pikovsky, and M. Rosenblum, Phys. Rev. Lett. **112**, 144103 (2014).
[7] M. J. Panaggio and D. M. Abrams, Nonlinearity **28**, R67 (2015).
[8] D. Battaglia, N. Brunel, and D. Hansel, Phys. Rev. Lett. **99**, 238106 (2007).

[9] R. Vicente, L. L. Gollo, C. R. Mirasso, I. Fischer, and P. Gorden, Proc. Natl. Acad Sci. USA **105**, 17157 (2008).

[10] N. C. Rattenborg, C. J. Amlaner, and S. L. Lima, Neurosci. Biobehav. Rev. **24**, 817 (2000).

[11] C. R. Laing and C. C. Chow, Neural Comput. **13**, 1473 (2001); C. R. Laing, W. C. Troy, B. Gutkin, and G. B. Ermentrout, SIAM J. Appl. Math. **63**, 62 (2002).

[12] K. Wiesenfeld, P. Colet, and S. H. Strogatz, Phys. Rev. Lett. **76**, 404 (1996).

[13] E. A. Martens, S. Thutupalli, A. Fourriére, and O. Hallatschek, Proc. Natl. Acad Sci. USA **110**, 10563 (2013).

[14] T. Kapitaniak, P. Kuzma, J. Wojewoda, K. Czolczynski, and Y. Maistrenko, Sci. Rep. **4**, 6379 (2014).

[15] N. Mazouz, G. Flätgen, and K. Krischer, Phys. Rev. E **55**, 2260 (1997).

[16] V. Garcia-Morales and K. Krischer, Phys. Rev. Lett. **100**, 054101 (2008).

[17] I. Omelchenko, Y. Maistrenko, P. Hövel, and E. Schöll, Phys. Rev. Lett. **106**, 234102 (2011).

[18] I. A. Shepelev, A. V. Bukh, G. I. Strelkova, T. E. Vadivasova, and V. S. Anishchenks, Nonlinear Dyn. **90**, 2317 (2017).

[19] A. V. Bukh, A. V. Slepnev, V. S. Anishchenko, and T. E. Vadivasova, Regul. Chaotic Dyn. **23**, 325 (2018).

[20] P. Chandran, R. Gopal, V. K. Chandrasekar, and N. Athavan, Chaos **29**, 053125 (2019).

[21] E. V. Rybalova, D. Y. Klyushina, V. S. Anishchenko, and G. I. Strelkova, Regul. Chaotic Dyn. **24**, 432 (2019).

[22] V. K. Chandrasekar, R. Gopal, A. Venkatesan, and M. Lakshmanan, Phys. Rev. E **90**, 062913 (2014).

[23] S. R. Ujjwal, N. Punetha, A. Prasad, and R. Ramaswamy, Phys. Rev. E **95**, 032203 (2017), and references therein.

[24] A. A. Khatun and H. H. Jafri, Commun. Nonlinear Sci. Numer. Simul. **95**, 105661 (2021).

[25] Y. C. Lai, C. Grebogi, J. A. Yorke, and S. C. Venkataramani, Phys. Rev. Lett. **77**, 55 (1996).

[26] S. Camargo, R. L. Viana, and C. Anteneodo, Phys. Rev. E **85**, 036207 (2012).

[27] S. R. Ujjwal, N. Punetha, R. Ramaswamy, M. Agarwal, and A. Prasad, Chaos **26**, 063111 (2016), and references therein.

[28] C. Bick, C. Kolodziejski, and M. Timme, Chaos **24**, 033138 (2014).

[29] J. Sieber, O. E. Omel'chenko, and M. Wolfrum, Phys. Rev. Lett. **112**, 054102 (2014).

[30] E. A. Martens, M. J. Panaggio, and D. M. Abrams, New J. Phys. **18**, 022002 (2016).

[31] I. Omelchenko, O. E. Omel'chenko, A. Zakharova, M. Wolfrum, and E. Schöll, Phys. Rev. Lett. **116**, 114101 (2016).

[32] I. Omelchenko, O. E. Omel'chenko, A. Zakharova, and E. Schöll, Phys. Rev. E **97**, 012216 (2018).

[33] I. Omelchenko, T. Hülser, A. Zakharova, and E. Schöll, Front. Appl. Math. Stat. **4**, 67 (2019).

[34] A. Gjurchinovski, E. Schöll, and A. Zakharova, Phys. Rev. E **95**, 042218 (2017).

[35] B. K. Bera, D. Ghosh, P. Parmananda, G. V. Osipov, and S. K. Dana, Chaos **27**, 073108 (2017).

[36] G. Ruzzene, I. Omelchenko, J. Sawicki, A. Zakharova, E. Schöll, and R. G. Andrzejak, Phys. Rev. E **102**, 052216 (2020).

[37] L. V. Gambuzza and M. Frasca, Phys. Rev. E **94**, 022306 (2016).

[38] C. Bick and Erik A. Martens, New J. Phys. **17**, 033030 (2015).

[39] T. Isele, J. Hizanidis, A. Provata, and P. Hövel, Phys. Rev. E **93**, 022217 (2016).

[40] G. Ruzzene, I. Omelchenko, E. Schöll, A. Zakharova, and R. G. Andrzejak, Chaos **29**, 051103 (2019).

[41] P. R. Sharma, A. Sharma, M. D. Shrimali, and A. Prasad, Phys. Rev. E **83**, 067201 (2011).

[42] P. R. Sharma, M. D. Shrimali, A. Prasad, and U. Feudel, Phys. Lett. A **377**, 2329 (2013).

[43] P. R. Sharma, A. Singh, A. Prasad, and M. D. Shrimali, Eur. Phys. J. **223**, 1531 (2014).

[44] P. R. Sharma, M. D. Shrimali, A. Prasad, N. V. Kuznetsov, and G. A. Lenov, Int. J. Bifurcation Chaos Appl. Sci. Eng. **25**, 1550061 (2015).

[45] L. M. Pecora and T. L. Carroll, Phys. Rev. Lett. **80**, 2109 (1998).

[46] L. Huang, Q. Chen, Y. C. Lai, and L. M. Pecora, Phys. Rev. E **80**, 036204 (2009).

[47] R. Sevilla-Escoboza, J. M. Buldú, A. N. Pisarchik, S. Boccaletti, and R. Gutiérrez, Phys. Rev. E **91**, 032902 (2015).

[48] F. Battiston, V. Nicosia, and V. Latora, Phys. Rev. E **89**, 032804 (2014).

[49] S. H. Strogatz, *Nonlinear Dynamics and Chaos: With Applications to Physics, Biology, Chemistry, and Engineering* (Perseus Books, New York, 1994).

[50] C. Sparrow, *The Lorenz Equations: Bifurcations, Chaos and Strange Attractors* (Springer, New York, 1982).

[51] The phases for single scroll attractors $C_{\mp}$ are calculated using $\phi_i = \tan^{-1}(y_i - y_0/x_i - x_0)$, where x_0, y_0 are centers of rotations, given by unstable fixed points $\mp[\beta(\gamma-1)]^{1/2}, \mp[\beta(\gamma-1)]^{1/2}$, respectively. For double scroll attractor C_0 we use $\phi_i = \tan^{-1}(z_i - z_0/u_i - u_0)$ with $u_i = (x_i^2 + y_i^2)^{1/2}$. z_0 and u_0 are mean values of the maxima and the minima of z_i and u_i variables, respectively.

[52] S. Rakshit, B. K. Bera, M. Perc, and D. Ghosh, Sci. Rep. **7**, 2412 (2017).

[53] For the frequency calculation of the motions on different attractors, we consider the time series of the variables x_i (for $C_{\mp}$) and $u_i = (x_i^2 + y_i^2)^{1/2}$ (for C_0), respectively.

[54] The differential equations are solved using a fourth-order Runge-Kutta method with an integration step of 0.01.

[55] J. Singha and N. Gupte, Phys. Lett. A **384**, 126225 (2020).

[56] V. Resmi, G. Ambika, and R. E. Amritkar, Phys. Rev. E **81**, 046216 (2010).

[57] L. Larger, B. Penkovsky, and Y. Maistrenko, Phys. Rev. Lett. **111**, 054103 (2013).

[58] S. Nkomo, M. R. Tinsley, and K. Showalter, Phys. Rev. Lett. **110**, 244102 (2013).

[59] D. Dudkowski, Y. Maistrenko, and T. Kapitaniak, Chaos **26**, 116306 (2016).

[60] Y. L. Maistrenko, A. Vasylenko, O. Sudakov, R. Levchenko, and V. L. Maistrenko, Int. J. Bifurcation Chaos Appl. Sci. Eng. **24**, 1440014 (2014), and references therein.

[61] R. Gopal, V. K. Chandrasekar, A. Venkatesan, and M. Lakshmanan, Phys. Rev. E **89**, 052914 (2014).

[62] A. E. Motter, S. A. Myers, M. Anghel, and T. Nishikawa, Nat. Phys. **9**, 191 (2013).

[63] F. Dörfler, M. Chertkov, and F. Bullo, Proc. Natl. Acad. Sci. USA **110**, 2005 (2013).

[64] B. K. Bera, D. Ghosh, and M. Lakshmanan, Phys. Rev. E **93**, 012205 (2016).

[65] H. Sakaguchi, Phys. Rev. E **73**, 031907 (2006).

[66] R. Karnatak, PLoS One **10**, e0142238 (2015).

[67] Similar qualitative results are observed for an ensemble of noisy Lorenz oscillators when delta-correlated Gaussian white noise $\sqrt{2D}\xi_i$ with unit variance and strength $\sqrt{2D} = 0.3$ is added to all three variables (x_i, y_i, z_i) of the system.